

# Direct Writing and Actuation of Three-Dimensionally Patterned Hydrogel Pads on Micropillar Supports\*\*

Lauren D. Zarzar, Philseok Kim, Mathias Kolle, C. Jeffrey Brinker, Joanna Aizenberg,\* and Bryan Kaehr\*

Many biological organisms employ micro- and nanoscale systems to actuate structural components with a high degree of spatial control. The resulting patterned or predetermined movement of the components gives rise to versatile biological materials with locally reconfigurable features and region-specific dynamic properties. On the molecular level, biological systems may regulate the availability of catalytic sites on enzymes by local reconfiguration of the protein structure, such as in allosteric modulation.<sup>[1]</sup> On the microscale, echinoderms use actuating pedicellariae for particle capture and release, and body cleaning,<sup>[2]</sup> and bacteria employ the movement of flagella to generate directional locomotion.<sup>[3]</sup> Squid use the mechanical expansion and contraction of

chromatophores to reversibly change color and pattern for camouflage and communication.<sup>[4]</sup> These systems provide inspiration for the development of artificial “smart” materials and surfaces with similar properties that respond autonomously and reversibly to environmental cues. Recently, such reversibly responsive materials, particularly those patterned or manipulated on the nano- and microscale, have been the subject of intense research<sup>[5]</sup> because of their promising impact in areas including sensors<sup>[6]</sup> and actuators,<sup>[7]</sup> microfluidic systems,<sup>[8]</sup> microelectromechanical systems,<sup>[9]</sup> and switchable surfaces with adaptive wettability, optical, mechanical, or adhesive properties.<sup>[5]</sup> In particular, hydrogels can be tailored to respond volumetrically to a wide variety of stimuli including temperature,<sup>[10]</sup> pH,<sup>[11]</sup> light,<sup>[12]</sup> and biomolecules (e.g., glucose),<sup>[13]</sup> and there has been a significant amount of research and applications devised for this class of materials in areas ranging from tissue engineering<sup>[14]</sup> to responsive photonics.<sup>[15]</sup>

We recently described a responsive and reversibly actuating surface based on a hybrid architecture consisting of passive polymeric structural (“skeletal”) elements embedded in and under the control of a responsive hydrogel layer (“muscle”) attached to a solid support.<sup>[16,17]</sup> While the volume change of the polymer muscle enables large-area, directional movement of skeletal elements, anchoring to a solid support imposes a serious constraint on the capacity for hydrogel expansion or contraction, thus limiting the extent of induced actuation of the structural elements. Moreover, this approach does not allow the formation of hydrogel islands that would induce localized actuation of selected areas and the associated regional changes in surface properties.

To expand the opportunities for integration of hydrogels in such composite systems, it would be advantageous to tailor not only the chemistry and swelling properties of the hydrogels but also the size, shape, and placement of the gel in relation to other system components. For example, well-defined, three dimensionally patterned, responsive hydrogel pads placed at the tips of micropillars with microscale control would enable nearly unrestricted gel swelling, both in and out of plane, which would locally actuate the pillars with more precise control over the movement of individual elements. While extensive research has been devoted to tailoring the swelling, chemical properties, and responsive behavior of hydrogels, less attention has been paid to the development of patterning protocols that would offer area-specific synthesis and 3D control over the micro- or nanoscale features of the gel. Many routes to defining hydrogel patterns have been explored including photolithography,<sup>[18]</sup> soft lithography,<sup>[19]</sup> and masking techniques,<sup>[20]</sup> but these 2D approaches lack

[\*] Prof. C. J. Brinker, Dr. B. Kaehr  
Advanced Materials Laboratory, Sandia National Laboratories  
1001 University Blvd. SE, Albuquerque, NM 87106 (USA)  
and  
Department of Chemical and Nuclear Engineering and Center for  
Micro-engineered Materials, University of New Mexico  
Albuquerque, NM 87106 (USA)  
E-mail: bjkaehr@sandia.gov  
L. D. Zarzar, Dr. P. Kim, Dr. M. Kolle, Prof. J. Aizenberg  
Department of Chemistry and Chemical Biology  
School of Engineering and Applied Sciences and  
Wyss Institute for Biologically Inspired Engineering  
Harvard University  
29 Oxford Street, Cambridge, MA 02138 (USA)  
E-mail: jaiz@seas.harvard.edu

[\*\*] We thank Dr. M. Aizenberg for discussions. This work was supported by the National Institute for Nano Engineering (NINE) program at Sandia National Laboratories; U.S. Department of Energy, Office of Basic Energy Sciences, and the Division of Materials Science and Engineering, grants DE-SC0005247 (responsive hydrogel actuation systems), DE-FG02-02-ER15368 (multi-photon lithography capabilities), and the Air Force Office of Scientific Research, grants 9550-10-1-0054 (hybrid materials and devices displaying a symbiotic relationship between the biotic and abiotic components), and FA9550-09-1-0669-DOD35CAP (responsive optics). Sandia is a multiprogram laboratory operated by Sandia Corporation, a Lockheed Martin Company, for the United States DOE's NNSA under contract DE-AC04-94AL85000. B.K. gratefully acknowledges the Sandia National Laboratories Truman Fellowship in National Security Science and Engineering and the Laboratory Directed Research and Development program for support. L.D.Z. thanks the Department of Defense for support through the National Defense Science and Engineering Graduate Fellowship Program, as well as the National Science Foundation for support through the Graduate Research Fellowship Program. M.K. acknowledges the Alexander von Humboldt-Foundation for support through a Feodor Lynen Research Fellowship.



Supporting information for this article is available on the WWW under <http://dx.doi.org/10.1002/anie.201102975>.

true control over gel features in 3D, thus limiting their application for localized microactuation.

Multiphoton lithography (MPL) has emerged as a prominent method for the fabrication of intricately 3D-structured materials with nanoscale precision.<sup>[21]</sup> Pulsed laser light is focused into a photosensitive reagent solution (e.g., photoresist) to initiate photochemical reactions by a multiphoton absorption process. This nonlinear excitation is restricted to regions of high photon density (i.e., proximal to the focal volume of a focused laser beam), thus enabling photochemical reactions, such as photopolymerization, to be confined to highly resolved 3D volumes on the order of approximately 1 fl. MPL has been commonly used with epoxy<sup>[21]</sup> and acrylic resins<sup>[21,22]</sup> that tend to be rigid when cured, thus allowing for creation of detailed and stable structures. However, much less attention has been given to MPL of soft materials such as hydrogels. While MPL has been used to polymerize acrylate-based<sup>[23–26]</sup> and protein-based hydrogels,<sup>[27]</sup> the stimuli-responsive behavior of these hydrogels has not been extensively investigated and only rarely were the swelling properties reported.<sup>[25–27]</sup>

Herein, we report an approach to directly write reversibly swelling pH- and temperature-responsive hydrogel patterns onto polymeric micropillars by using MPL and examine their localized actuation. For this work, we chose two common and widely studied polymers: temperature-responsive poly(*N*-isopropylacrylamide) (PNIPAAm) and pH-responsive poly(acrylic acid-*co*-acrylamide) (poly(AAc-*co*-AAM)). In a typical experiment, polymer precursors were dissolved in ethylene glycol (40 % w/w) in the presence of a UV-curable

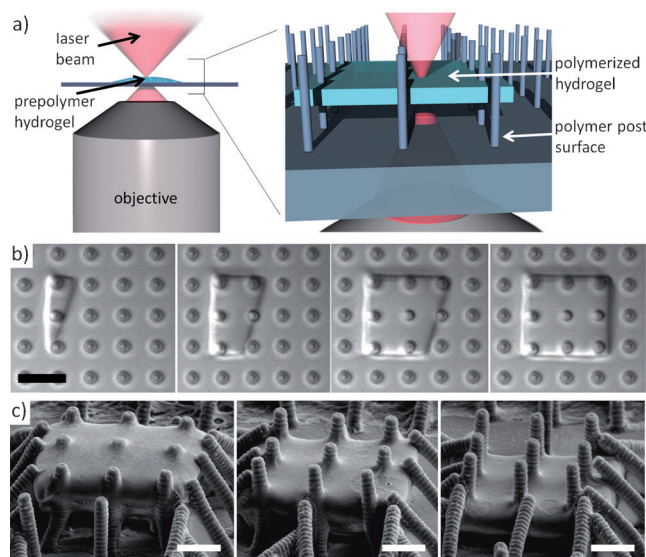


**Figure 1.** a) Experimental setup for localized synthesis of MPL hydrogels onto micropillars (height = 10  $\mu\text{m}$ , pitch = 8  $\mu\text{m}$ , diameter = 1.5  $\mu\text{m}$ ). b) Image sequence of multiphoton-induced polymerization to form a thin hydrogel structure attached to the pillars (see Supporting Movie 1). Scale bar: 10  $\mu\text{m}$ . c) SEM images showing fabricated hydrogel structures placed precisely along the top, center, and bottom of the posts. The thickness of the hydrogel pads is approximately 2  $\mu\text{m}$  made by two passes of the scanning laser beam. Scale bars: 5  $\mu\text{m}$ .

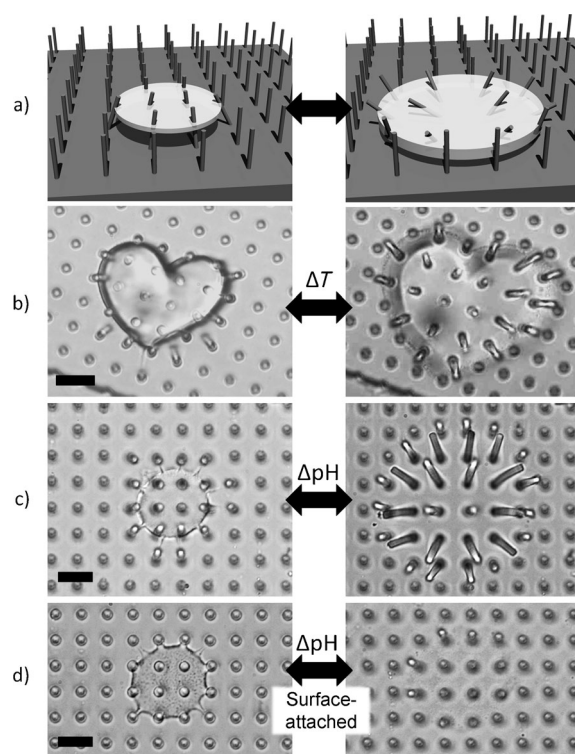


**Figure 2.** a) Schematic showing the deflection of the flexible pillars by tip-attached hydrogel swelling. Optical microscope images of the contracted and swollen states of b) temperature-responsive hydrogel (at  $T > 30^\circ\text{C}$  and  $T < 30^\circ\text{C}$ ) and c) pH-responsive hydrogel (at  $\text{pH} < 4.25$  and  $\text{pH} > 4.25$ ) are shown. d) pH-responsive gel under the same conditions as (c) but fabricated at the base of the pillars and attached to the basal surface. Scale bars: 10  $\mu\text{m}$ .

photoinitiator (1 % w/w), such as bis(2,4,6-trimethylbenzoyl)-phenylphosphine oxide (Irgacure 819), which shows significant absorption around 400 nm to enable two-photon excitation using 750–800 nm pulsed laser light operating at relatively low average powers. The ethylene glycol was exchanged with water after fabrication. As shown in Figure 1a, the hydrogel precursor solution is placed on a micropillar surface and the laser is passed through an objective lens and into the solution; polymerization occurs proximal to the laser focus as it is scanned across the sample (Figure 1b) and hydrogel structures of user-defined shapes<sup>[28]</sup> can be written directly on the polymer bristles at arbitrary distances above the basal surface (Figure 1c; see the Supporting Information for experimental details, and Supporting Movie 1).

Figure 2a,b show a schematic of the actuation cycle followed by the optical micrographs of a heart-shaped PNIPAAm gel, fabricated at the micropillar tips, which we observed to have a phase transition at around  $30^\circ\text{C}$  switching between the contracted ( $T > 30^\circ\text{C}$ ) and swollen ( $T < 30^\circ\text{C}$ ) state. Poly(AAc-*co*-AAM) hydrogels, which are pH responsive and exhibit a volume phase transition near the  $\text{pK}_\text{a}$  value of acrylic acid (4.25),<sup>[29]</sup> were attached to the flexible micropillars and fabricated by using the same procedure (Figure 2c). These hydrogels (both temperature- and pH-responsive) could be swollen and contracted rapidly (within seconds; see Supporting Movie 2) for dozens or more cycles with little

deformation in gel structure. Importantly, suspending the hydrogel on the flexible pillars above the substrate surface allows the gel to swell and contract significantly without being constrained by surface attachment. For the thin suspended hydrogel pads, absolute expansion and contraction is greatest along the axes parallel to the surface plane, thus actuating the flexible pillars outward or inward (Figure 2b,c). To demonstrate the importance of suspending the gel, we fabricated a pH-responsive gel attached to the basal surface (Figure 2d) but otherwise identical to the gel shown in Figure 2c. The degree of lateral swelling in response to pH change is significantly constrained because of the surface attachment, and the actuation of the pillars is negligible.

We envision use of these 3D-patterned hydrogels as muscle components to actuate artificial filamentous surfaces (or other flexible structures) with a high level of control. To guide these efforts, we investigated how the swelling of the disk-shaped MPL-patterned poly(AAc-co-AAm) hydrogel

swelling influences the bending of the epoxy pillars across a range of pH values between 2 and 8.8 (Figure 3a). Bending angles for three posts (chosen in a single row across the diameter of the disk) exhibit a sharp transition between pH 4–5 in correlation with the expected pH range for the volume phase transition. However, the absolute bending angle in either the swollen or contracted state ultimately depends on the position of each post; bending angles between  $-20^\circ$  and greater than  $70^\circ$  were accessible for posts located near the outer edge of the hydrogel, but the range was much smaller for posts near the center of the hydrogel disk. Assuming that the primary force exerted upon the posts arises from an outwardly expanding hydrogel located near the tips, the forces exerted upon the microposts were approximated using Equation (1):

$$\text{force} = \frac{3\pi E r^4}{4h^3} D \quad (1)$$

where  $E$  is the Young's modulus of the glycidyl methacrylate modified epoxy (1.5 GPa),<sup>[16]</sup>  $r$  is the radius of the posts ( $0.75\ \mu\text{m}$ ),  $h$  is the height of the posts ( $10\ \mu\text{m}$ ), and  $D$  is the distance to which the tip of each post is deflected from its initial position. The forces mapped over the surface plane of the disk in Figure 3b indicate that forces on the order of  $\mu\text{N}$  were generated near the edge of the swelled gel and are sufficient for microscale manipulations where viscous forces on the order of pN must be overcome.<sup>[30]</sup> The ability to apply directed forces and dictate filament trajectory from its relative position within the gel provides a foundation to begin to explore actuation schemes over larger distances, for instance, to direct or trap particles with environmental cues using a cilia-like mechanism.

The ability to synthesize interacting hydrogels that respond to different stimuli should enable the realization of

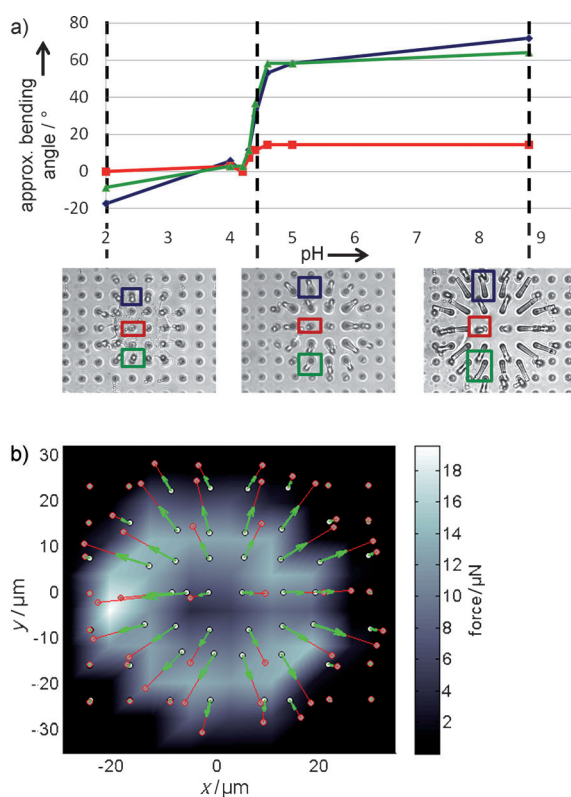


**Figure 3.** a) Plot of approximate bending angles of pillars that support a pH-responsive hydrogel pad as a function of pH value, where a negative angle represents the pillar bending inward toward the center of the gel, and a positive angle represents outwardly bending pillars. Posts near the center of the structure (red) show little change in bending. Posts near the edge of the hydrogel (blue and green) bend to very large angles ( $> 70^\circ$ ). b) The displacement of the posts was used to generate a force map of the gel. White circles indicate the initial positions of the tips of the pillars when the gel is contracted, and red circles indicate the position of the tips of the pillars when the gel is swollen. Red lines connect the initial and final positions. Green arrows represent the amount of force normalized to the largest force experienced by a pillar in the system. The background color map visualizes the extent of the net force exerted on the pillars in different areas of the gel.

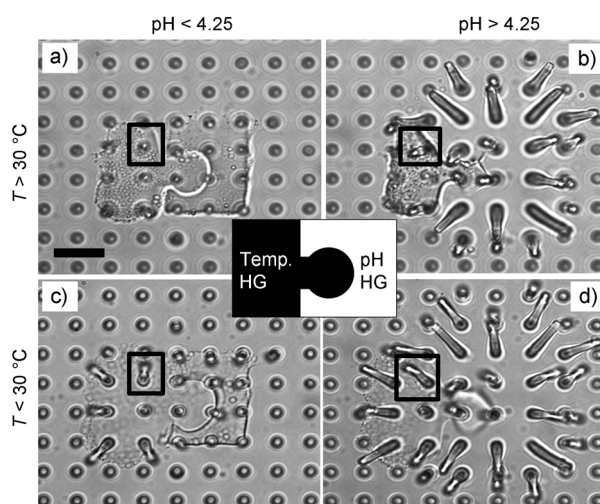


**Figure 4.** Schematic showing temperature- and pH-responsive hydrogels (HGs) fabricated in proximity as interlocking puzzle-piece shapes (center). Optical microscope images at each temperature and pH combination are shown (a–d). The black outline highlights an exemplary post as it is bent at four different angles and directions depending on the combination of conditions. Scale bar:  $10\ \mu\text{m}$ .



more complex behavior that is not achievable with uniform hydrogel muscles. As shown in Figure 4, the pH-responsive hydrogel and temperature-responsive hydrogel were patterned sequentially as interlocking puzzle pieces. Each hydrogel could be stimulated in an independent manner by changing the combination of pH and temperature. Pillars that had a temperature-responsive hydrogel on one side and pH-responsive hydrogel on the other, near the interface of the gels, could therefore be actuated to four stable configurations; one such post is highlighted in Figure 4. The shape of the hydrogel at the interface (the interlocking part of the pieces) could be compressed or expanded by the response of the neighboring gel. In Figure 4, for example, comparison of (a) to (b) and (c) to (d) illustrates that at constant temperatures but varying pH value, the extruding part of the temperature-responsive hydrogel piece is compressed beyond its equilibrium state by an expanding pH-responsive hydrogel. Similarly, upon comparison of (a) to (c) and (b) to (d), we see that the shape of the pH-responsive hydrogel at the interlocking segment is expanded at constant pH but varying temperature. The ability to precisely pattern interacting hydrogels of varying responsivity may provide opportunities for the design of systems that exhibit predictive and programmable responses for different combinations of environmental conditions; reconfiguration of structures may now have more than a single “muscle” that controls actuation and induces complex movement of structural elements.

A potent feature of responsive hydrogels is their ability to dynamically adjust and tune the functional density of any chemical moiety in the gel by the volume phase transition. To demonstrate this capability in MPL-generated gels, we copolymerized a fluorescent polymerizable rhodamine monomer, methacryloxyethyl thiocarbamoyl rhodamine B, with the

pH-responsive hydrogel and patterned the gel on the micropillars (Figure 5). We used poly(AAc-co-AAm) because of its large swelling response and rhodamine B because its fluorescence is insensitive to changes in pH value over the range needed for the swelling response. Expansion and contraction of the fluorophore-modified hydrogel conferred substantial changes in the fluorescence intensity. In particular, suspending the gel above the substrate surface through attachment along the tips of the pillars (as is shown in Figure 1c, left) provided excellent “on/off” behavior of the optical signal (see Supplementary Movie 3). The significant changes in fluorescence intensity were attributed to the extreme volume phase transition of the unconstrained hydrogel and its influence on the effective density of the fluorophore within the gel volume. Using multiphoton excitation (MPE) point measurements, which provide a means to probe a fixed volume of the hydrogel in both its expanded and contracted states, we measured an approximate 20-fold increase in the density of rhodamine molecules within gels similar to those pictured in Figure 5. As a result, the message written with the hydrogel in Figure 5a is clearly seen at pH values less than 4.25 and is effectively “erased” at pH values greater than 4.25. Similarly, additional functional components including nanoparticles,<sup>[31]</sup> peptides,<sup>[32]</sup> and DNA,<sup>[33]</sup> can be readily incorporated into these gels and should expand the opportunities for dynamic optical materials, sensors, and catalytic systems<sup>[34]</sup> in which the density and availability of the active sites is tuned by gel response.

In conclusion, we have described a synthetic route to fabricate arbitrary 3D shapes of temperature- and pH-responsive hydrogels by using MPL. This procedure allows hydrogels to be precisely positioned in a suspended state on high-aspect-ratio micropillar structures giving rise to significant gel expansion without the surface constraint that typically results from traditional patterning methods in which the gel is attached to the basal surface. The bending angle and actuation direction of microposts are shown to depend on their relative lateral positions (i.e., center versus edge) within the swelling gel, thus providing a means to direct the movement of post structures with a high degree of tunability. We have shown that this approach makes it possible to pattern interlocking, interacting hydrogels that respond to different stimuli and thus to develop unique, complex gel and structural interactions by orthogonal environmental cues. Additionally, hydrogels can be further functionalized, for instance, by introducing a polymerizable fluorophore to generate an optical readout based on the actuation-induced concentration change. MPL-patterned responsive hydrogels that incorporate chemical, optical, and catalytic<sup>[34]</sup> or enzymatic<sup>[35]</sup> functions will provide great opportunities to develop multicomponent chemical reaction, sensing, and diagnostic systems. Although we describe micropatterned 3D “muscle-like” materials integrated with relatively simple micropillar components, similar 3D microactuation is achievable for more complex “skeletal” structures that can be fabricated using common MPL acrylic- and epoxy-based precursors. These studies can be further extended to 3D patterning of other common responsive gels that are based on similar polymerization chemistry, thus tuning the responsivity

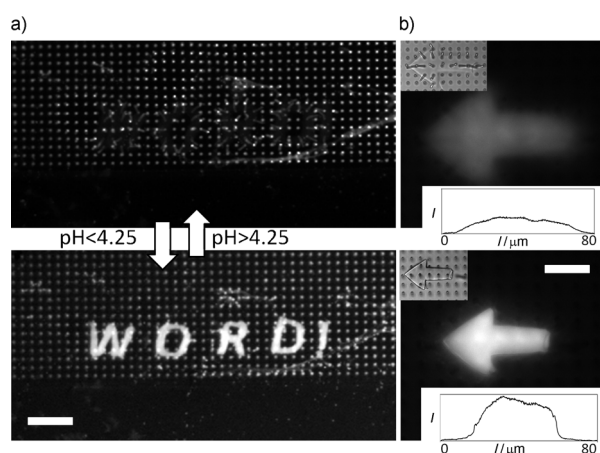


**Figure 5.** Fluorescence microscopy images demonstrating fast and reversible appearance and disappearance of written messages arising from the change in concentration density of a rhodamine dye which was incorporated into a pH-responsive hydrogel. a) Contraction of the hydrogel in acid increases the fluorescence signal to reveal the written message “word!” (see Supporting Movie 3). Scale bar: 40  $\mu\text{m}$ . b) Contraction of the hydrogel in acid reveals the arrow symbol. Upper insets show differential interference contrast (DIC) images of the gel. Lower insets show the fluorescence intensity profile along the length of the arrow normalized to the bit depth of the fluorescence image. Scale bar: 20  $\mu\text{m}$ .

of the system for various environments. This synthetic procedure, with its significant capabilities for extensions of structural as well as hydrogel variability, should enable the exploration of autonomous micro/nanoactuators both inspired by biological systems and creatively engineered.

Received: April 29, 2011

Published online: August 22, 2011

**Keywords:** actuation · gels · hybrid materials · micropatterning · multiphoton lithography

- [1] J. Monod, J.-P. Changeux, F. Jacob, *J. Mol. Biol.* **1963**, 6, 306.
- [2] M. Ghyoot, C. D. Ridder, M. Jangoux, *Zoomorphology* **1987**, 106, 279.
- [3] R. M. Macnab, *J. Bacteriol.* **1999**, 181, 7149.
- [4] R. L. Sutherland, L. M. Mäthger, R. T. Hanlon, A. M. Urbas, M. O. Stone, *J. Opt. Soc. Am.* **2008**, 25, 588.
- [5] M. A. C. Stuart, W. T. S. Huck, J. Genzer, M. Müller, C. Ober, M. Stamm, G. B. Sukhorukov, I. Szleifer, V. V. Tsukruk, M. Urban, F. Winnik, S. Zauscher, I. Luzinov, S. Minko, *Nat. Mater.* **2010**, 9, 101.
- [6] H. Saito, Y. Takeoka, M. Watanabe, *Chem. Commun.* **2003**, 2126.
- [7] A. Sidorenko, T. Krupenkin, A. Taylor, P. Fratzl, J. Aizenberg, *Science* **2007**, 315, 487.
- [8] D. J. Beebe, J. S. Moore, J. M. Bauer, Q. Yu, R. H. Liu, C. Devadoss, B.-H. Jo, *Nature* **2000**, 404, 588.
- [9] G. P. A. Richter, *Adv. Mater.* **2009**, 21, 979.
- [10] H. G. Schild, *Prog. Polym. Sci.* **1992**, 17, 163.
- [11] X. Zhou, L. Weng, Q. Chen, J. Zhang, D. Shen, Z. Li, M. Shao, J. Xu, *Polym. Int.* **2003**, 52, 1153.
- [12] M. Irie, D. Kunwatchakun, *Macromolecules* **1986**, 19, 2476.
- [13] K. Kataoka, H. Miyazaki, M. Bunya, T. Okano, Y. Sakurai, *J. Am. Chem. Soc.* **1998**, 120, 12694.
- [14] B. Jeong, A. Gutowska, *Trends Biotechnol.* **2002**, 20, 305.
- [15] J. Ge, Y. Yin, *Angew. Chem.* **2011**, 123, 2; *Angew. Chem. Int. Ed.* **2011**, 50, 2.
- [16] P. Kim, L. D. Zarzar, X. Zhao, A. Sidorenko, J. Aizenberg, *Soft Matter* **2010**, 6, 750.
- [17] L. D. Zarzar, P. Kim, J. Aizenberg, *Adv. Mater.* **2011**, 23, 1442.
- [18] S. J. Bryant, K. D. Hauch, B. D. Ratner, *Macromolecules* **2006**, 39, 4395.
- [19] T. Yu, C. K. Ober, *Biomacromolecules* **2003**, 4, 1126.
- [20] D. Y. Wong, D. R. Griffin, J. Reed, A. M. Kasko, *Macromolecules* **2010**, 431, 2824.
- [21] C. N. LaFratta, J. T. Fourkas, T. Baldacchini, R. A. Farrer, *Angew. Chem.* **2007**, 119, 6352; *Angew. Chem. Int. Ed.* **2007**, 46, 6238.
- [22] T. Baldacchini, C. N. LaFratta, R. A. Farrer, M. C. Teich, B. E. A. Saleh, M. J. Naughton, J. T. Fourkasa, *J. Appl. Phys.* **2004**, 95, 6072.
- [23] P. J. Campagnola, D. M. Delguidice, G. A. Epling, K. D. Hofacker, A. R. Howell, J. D. Pitts, S. L. Goodman, *Macromolecules* **2000**, 33, 1511.
- [24] S. Li, L. Li, F. Wub, E. Wang, *J. Photochem. Photobiol. A* **2009**, 203, 211.
- [25] S. J. Jhaveri, J. D. McMullen, R. Sijbesma, L.-S. Tan, W. Zipfel, C. K. Ober, *Chem. Mater.* **2009**, 21, 2003.
- [26] T. Watanabe, M. Akiyama, K. Totani, S. M. Kuebler, F. Stellacci, W. Wenseleers, K. Braun, S. R. Marder, J. W. Perry, *Adv. Funct. Mater.* **2002**, 12, 611.
- [27] B. Kaehr, J. B. Shear, *Proc. Natl. Acad. Sci. USA* **2008**, 105, 8850.
- [28] R. Nielson, B. Kaehr, J. B. Shear, *Small* **2009**, 5, 120.
- [29] S. K. De, N. R. Aluru, *J. Microelectromech. Syst.* **2002**, 11, 544.
- [30] B. Behkam, M. Sitti, *Appl. Phys. Lett.* **2007**, 90, 023902.
- [31] M. Oishi, H. Hayashi, T. Uno, T. Ishii, M. Iijima, Y. Nagasaki, *Macromol. Chem. Phys.* **2007**, 208, 1176.
- [32] K. L. Heredia, Z. P. Tolstyka, H. D. Maynard, *Macromolecules* **2007**, 40, 4772.
- [33] J. Liu, *Soft Matter* **2011**, 7, 6757.
- [34] K. Okeyoshi, R. Yoshida, *Adv. Funct. Mater.* **2010**, 20, 708.
- [35] K. Podual, F. J. Doyle III, N. A. Peppas, *J. Controlled Release* **2000**, 67, 9.